10 Quantum Monte Carlo Methods for Fermion-Boson Problems

Fakher F. Assaad
Institut für Theoretische Physik und Astrophysik
Universität Würzburg
Am Hubland, D-97074 Würzburg

Contents

E. Pavarini, E. Koch, A. Lichtenstein, and D. Vollhardt (eds.)
DMFT: From Infinite Dimensions to Real Materials
Modeling and Simulation Vol. 8
Forschungszentrum Jülich, 2018, ISBN 978-3-95806-313-6
http://www.cond-mat.de/events/correl18

1 Introduction

Fermion-boson systems play an important role in many domains of physics. An example in the solid state is the electron-phonon problem that leads to many collective phenomena such as superconductivity [1–3], charge density waves [4,5], and topological effects [6,7]. In high energy physics, especially lattice gauge theories, the bosonic modes account for the gauge fields that mediate interactions between fermion matter fields. Recently a number of so called designer Hamiltonians have been introduced to describe a variety of phases and quantum phase transitions [8–14]. As we will see, these models all fall in the class of electron-boson Hamiltonians and are designed to capture the essential physics at hand without encountering the infamous sign problem. In doing so, nematic and ferromagnetic quantum phase transitions in metals as well as topological states of matter can be studied unbiasedly and on *large* system sizes.

In a former issue of these lecture notes [15] we had already considered this problem, but for the special case of non-interacting bosons coupled to interacting fermions. We had adopted an action based formalism and integrated-out the bosonic degrees of freedom in favor of a fermion-only problem, albeit with retarded interactions. Such action-based problems are conveniently solved within the continuous-time interaction-expansion (CT-INT) algorithm [16, 17] that is very powerful for a variety of models including the electron-phonon problem [18–20]. Integrating-out the phonons certainly facilitates things and local sampling strategies turn out to be efficient in many cases. However the approach has some drawbacks. i) The computational effort scales as the cube of the number of (interacting) fermion sites, N, times the cube of the inverse temperature β. Even if the pre-factor of this scaling law is small, it will ultimately be hard to reach very large system sizes. For example, for the one dimensional Holstein model, a very efficient directed loop algorithm for retarded interactions has been formulated that clearly out-preforms the CT-INT approach [21]. ii) Integrating-out the bosons actually can generate a negative sign problem which would not occur in formulations where the bosons are explicitly taken into account. This happens in the two dimensional case [22]. iii) Finally, integrating-out the bosonic modes is only possible if they do not interact.

In this review we will discuss various formulations of the auxiliary-field QMC (AFQMC) approach for electron-boson systems. We will concentrate only on models where the so called negative sign problem is absent, such that the problem reduces to the sampling of a non-local probability distribution in a high dimensional space. There has recently been tremendous progress in defining the class of problems that can be solved without encountering the negative sign problem [23–26]. The models we will define here are certainly inspired from these new insights. In particular we will start with a *many body classic*, the Su-Schrieffer-Heeger (SSH) model [6] introduced to study soliton excitations in polyacetylene. Here we will consider the two dimensional case, and show that in limiting cases the model is equivalent to Z_2 lattice gauge theories where the Gauss law is dynamically imposed at low temperatures. Models with Z_2 symmetries, local or global, are more easily formulated by considering Ising bond variables coupled to fermions. This class of problems shows extremely rich phase diagrams [8–14] and it is of great interest to find efficient algorithms to simulate them.

Since, as mentioned above, the infamous negative sign problem is absent in the class of models we will consider, the reader could ask the pertinent question: what is then so hard? It is the sampling. For fermion-boson problems, the major issue that we will encounter are very long autocorrelation times [27] when adopting simple single spin-flip updates. Historically for the Ising model cluster updates circumvent critical slowing down [28]. The beauty of these algorithms is that, as one approaches the critical point, blocks of spins, the size of which tracks the correlation length, are flipped and accepted with unit probability. Cluster algorithms have been formulated for problems where the action is local. For fermion systems the action is highly non-local and defining cluster algorithms for fermions is an open question.
Faced with this challenge, one can progress in various ways. One approach is to use concepts of machine learning, more specifically so called self-learning algorithms [29, 30]. Here the idea is to define a simpler *auxiliary* model on the same configuration space as the original one endowed with a set of free parameters. Assume that one has a representative set of configurations and associated weights for the original model, then we can train (i.e. tune the free parameters) of the auxiliary model, so as to at best reproduce the data set of configurations and weights. If this step is successful, one will then use the auxiliary model to propose new configurations.
In this review we will adopt other strategies, presented in [31], to argue that so called hybrid molecular-dynamics sampling is the method of choice for a class of electron-boson problems. We will combine two approaches: the Blankenbecler-Scalapino-Sugar (BSS) formulation [32] of the AFQMC supplemented by a hybrid molecular-dynamics sampling of the fields [33, 34].
This review is organized as follows. In the next section we will first introduce a set of models, that are all free of the negative sign problem and that fall in the category of fermion-boson problems. They all have in common an $\mathrm{O}(2N)$ symmetry where N corresponds to the number of fermion flavors. In Sec. 3 we will derive in all details the equations required to formulate the AFQMC. Our approach will be based on the Grassmann algebra, aspects of which are reviewed in Appendix A. It is however beyond the scope of this monograph to discuss the detailed implementation of the algorithm. For this, we refer the reader to [35] and to [36] for a generic implementation of the AFQMC. In the last section, we will give some reasons why single spin-flip updates suffer from long autocorrelation times. To circumvent this problem we will discuss alternative forms of sampling strategies, in particular Langevin and hybrid molecular dynamics. We have tested favorably these ideas in Ref. [31]. Finally, we give our conclusions.

2 Model systems

In this section we review a number of models that show extremely rich phase diagrams with exotic phases and quantum phase transitions. They are all related to each other, and fall in the greater class of fermion-boson models. We will start with the canonical Su-Schrieffer-Heeger (SSH) model and show that in limiting cases it maps onto unconstrained Z_2 lattice gauge theories. Using duality transformations we can map Z_2 lattice gauge theories, in the absence of *visons*, to Falikov-Kimball models [37]. Finally, breaking the local Z_2 symmetry to a global one, naturally leads to the problem of fermions coupled to an Ising model in a transverse field.

2.1 The Su-Schrieffer-Heeger model

In the one-dimensional case, the SSH model describes solitonic excitations in polyacetylene [6]. In this dimension, the model can be solved efficiently with the CT-INT approach [38, 15]. In higher dimensions the phase diagram of the model is essentially unknown and the CT-INT approach suffers form a negative sign problem. The model is given by

$$\hat{H} = \hat{H}_{\mathrm{el}} + \hat{H}_{\mathrm{ph}} + \hat{H}_{\mathrm{ep}}. \tag{1}$$

Here

$$\hat{H}_{\mathrm{el}} = -t \sum_{\langle i,j\rangle,\sigma} \left(\hat{c}^{\dagger}_{i,\sigma} \hat{c}_{j,\sigma} + \hat{c}_{j,\sigma} \hat{c}^{\dagger}_{i,\sigma} \right), \tag{2}$$

is the kinetic energy and $\langle i,j\rangle$ denotes the nearest neighbors of a square lattice. $\hat{c}^{\dagger}_{i,\sigma}$ creates an electron in a Wannier state centered around lattice site i, and with flavor index σ. We allow the flavor index to take any integer value. Remarkably, this will not introduce a negative sign problem. Harmonic oscillators on links account for the lattice vibrations,

$$\hat{H}_{\mathrm{ph}} = \sum_{\langle i,j\rangle} \left(\frac{\hat{p}^2_{\langle i,j\rangle}}{2m} + \frac{m\omega^2}{2} \hat{x}^2_{\langle i,j\rangle} \right), \tag{3}$$

with $\hat{p}, \hat{x}$ being the canonical conjugate momentum and position operators. The electron-phonon coupling leads to a modulation of the hopping matrix element:

$$\hat{H}_{\mathrm{ep}} = g \sum_{\langle i,j\rangle,\sigma} \hat{x}_{\langle i,j\rangle} \left(\hat{c}^{\dagger}_{i,\sigma} \hat{c}_{j,\sigma} + \hat{c}^{\dagger}_{j,\sigma} \hat{c}_{i,\sigma} \right) \tag{4}$$

with coupling strength g. To simplify the notation we label bond indices as

$$b := \langle i,j\rangle\,, \tag{5}$$

and introduce the bond hopping as

$$\hat{K}_b := \sum_{\sigma} \left(\hat{c}^{\dagger}_{i,\sigma} \hat{c}_{j,\sigma} + \hat{c}^{\dagger}_{j,\sigma} \hat{c}_{i,\sigma} \right). \tag{6}$$

2.2 Unconstrained lattice gauge theories

Unconstrained lattice gauge theories can be derived from the above SSH model, provided that we set the hopping matrix element to zero. This step certainly violates the harmonic approximation central to the very definition of phonons. Nevertheless the model is well defined, and the flexibility inherent to systems of cold atoms trapped in optical lattices may offer possible realizations of such systems [39]. Introducing the boson operators,

$$\hat{b}^{\dagger}_{\langle i,j\rangle} = \frac{\omega m \hat{x}_{\langle i,j\rangle} - i\hat{p}_{\langle i,j\rangle}}{\sqrt{2\omega m}}, \tag{7}$$

we can rewrite the model as

$$\hat{H}_{Z_2} = g\sqrt{\frac{1}{2\omega m}} \sum_{\langle i,j \rangle} \left(\hat{b}^\dagger_{\langle i,j \rangle} + \hat{b}_{\langle i,j \rangle} \right) \hat{K}_{\langle i,j \rangle} + \omega \sum_b \hat{b}^\dagger_{\langle i,j \rangle} \hat{b}_{\langle i,j \rangle}. \tag{8}$$

Due to the lack of a direct hopping term, the above model acquires a local symmetry. In particular, the boson parity on the four links emanating from site i times the fermion parity on the site is a local conserved Ising variable. That is, for

$$\hat{Q}_i = (-1)^{\hat{n}^b_{\langle i,i+a_x \rangle} + \hat{n}^b_{\langle i,i-a_x \rangle} + \hat{n}^b_{\langle i,i+a_y \rangle} + \hat{n}^b_{\langle i,i-a_y \rangle}} (-1)^{\hat{n}^c_i} \tag{9}$$

we have

$$\left[\hat{Q}_i, \hat{H}_{Z_2} \right] = 0 \quad \text{with} \quad \hat{Q}_i^2 = 1 \quad \text{and} \quad \left[\hat{Q}_i, \hat{Q}_j \right] = 0. \tag{10}$$

In the above, $\hat{n}^b_{\langle i,j \rangle} = \hat{b}^\dagger_{\langle i,j \rangle} \hat{b}_{\langle i,j \rangle}$ and $\hat{n}^c_i = \sum_\sigma \hat{c}^\dagger_{i,\sigma} \hat{c}_{i,\sigma}$. $\hat{Q}_i$ defines a Z_2 charge that is conserved locally in space but not in time.[1] To see this we note that

$$\left[\hat{Q}_i, \hat{b}_{\langle n,m \rangle} \right] = 2\hat{Q}_i \hat{b}_{\langle n,m \rangle} \left(\delta_{i,m} + \delta_{i,n} \right) \quad \text{and} \quad \left[\hat{Q}_i, \hat{c}_{j,\sigma} \right] = 2\hat{Q}_i \hat{c}_{j,\sigma} \, \delta_{i,j} \tag{11}$$

such that

$$\langle \hat{c}_i \hat{c}^\dagger_j \rangle = \delta_{i,j} \tag{12}$$

and a similar equation holds for the bosons. The above merely states that since the electron carries a Z_2 charge that is locally conserved in space, the equal time propagator between different lattice sites has to vanish. The difference between the above Hamiltonian and lattice gauge theories is that the Z_2 charge is not conserved along the imaginary time axis: $\langle \hat{c}_i(\tau) \, \hat{c}^\dagger_j \rangle = \delta_{i,j}$ with $\hat{c}_i(\tau) = e^{\tau \hat{H}} \, \hat{c}_i \, e^{-\tau \hat{H}}$. Such so called unconstrained gauge theories, where the Gauss law is not imposed, have recently attracted considerable interest [10, 40, 41].

The above model has the same symmetries as a Z_2 lattice gauge theory and the exact relationship can be obtained by restricting the boson Hilbert space to two states: the vacuum and the first excited state, $\left\{ |0\rangle, |1\rangle = \hat{b}^\dagger |0\rangle \right\}$. This reduction of the Hilbert space amounts to replacing the soft core bosons by hard core ones, $\hat{b}^\dagger \hat{b}^\dagger = 0$, which is certainly a valid approximation in the antiadiabatic limit, $\omega \to \infty$. Next, we define Ising variables: $|\pm\rangle = \frac{1}{\sqrt{2}} \left(|1\rangle \pm |0\rangle \right)$ such that for

$$\hat{X}_{\boldsymbol{b}} = 2\hat{b}^\dagger_{\boldsymbol{b}} \hat{b}_{\boldsymbol{b}} - 1, \quad \hat{Z}_{\boldsymbol{b}} = \hat{b}^\dagger_{\boldsymbol{b}} + \hat{b}_{\boldsymbol{b}} \tag{13}$$

$$\hat{X}_{\boldsymbol{b}} |\pm\rangle = |\mp\rangle \text{ and } \hat{Z}_{\boldsymbol{b}} |\pm\rangle = \pm |\pm\rangle. \tag{14}$$

With this reading, the SSH model reduces, up to a constant, to

$$\hat{H}_{Z_2} = \sum_{\langle i,j \rangle} \hat{Z}_{\langle i,j \rangle} \hat{K}_{\langle i,j \rangle} - h \sum_{\langle i,j \rangle} \hat{X}_{\langle i,j \rangle} \tag{15}$$

Here we have set $g/\sqrt{2\omega m} = 1$ such that $h = -g^2/4m$. Under the above mapping the conserved Z_2 charge transforms to

$$\hat{Q}_i = \hat{X}_{\langle i,i+a_x \rangle} \hat{X}_{\langle i,i-a_x \rangle} \hat{X}_{\langle i,i+a_y \rangle} \hat{X}_{\langle i,i-a_y \rangle} (-1)^{\hat{n}^c_i}. \tag{16}$$

[1] This stems from the fact that the constraint, say $\hat{Q}_i = 1$, is not imposed on the Hilbert space.

The above model has captured a considerable amount of interest [10, 11, 14]. It is extremely simple and hosts deconfined and confined phases of matter as well as exotic quantum phase transitions (see Fig. 1).

2.3 Duality transformations and a Falikov-Kimball model

In interacting systems, interaction terms that do not break the macroscopic symmetries of the model will generically be dynamically generated. For example in the functional renormalization group [42] flow, one will be able to study the dynamically generated interactions in various channels. Let us follow this idea in the context of the above unconstrained lattice gauge theories. On a square lattice, the flux term

$$\hat{H}_F = F \sum_i \hat{Z}_{\langle i,i+a_x\rangle}\, \hat{Z}_{\langle i+a_x,i+a_x+a_y\rangle}\, \hat{Z}_{\langle i+a_x+a_y,i+a_y\rangle}\, \hat{Z}_{\langle i+a_y,i\rangle} \tag{17}$$

does not break any symmetries of the model and will hence be dynamically generated. In fact, for $h = 0$ in Eq. (15), the Ising fields will order so as to accommodate a π-flux ($\hat{Z}_{\langle i,i+a_x\rangle}$ $\hat{Z}_{\langle i+a_x,i+a_x+a_y\rangle}\, \hat{Z}_{\langle i+a_x+a_y,i+a_y\rangle}\, \hat{Z}_{\langle i+a_y,i\rangle} = -1$) per plaquette [10, 43], so as to dynamically generate Dirac fermions. A Falikov-Kimball model [37] is related to Eq. (15) in the sector where the flux per plaquette vanishes

$$\hat{Z}_{\langle i,i+a_x\rangle}\, \hat{Z}_{\langle i+a_x,i+a_x+a_y\rangle}\, \hat{Z}_{\langle i+a_x+a_y,i+a_y\rangle}\, \hat{Z}_{\langle i+a_y,i\rangle} = 1. \tag{18}$$

This corresponds to the zero *vison*, i.e., plaquettes with π-flux, sector. Let us work in a basis where $\hat{Z}$ is diagonal and consider a zero vison state. The transverse Ising field term creates a pair of visons on neighboring plaquettes and thereby violates the zero vison constraint. The first non-trivial term that complies with the constraint reads

$$\tilde{h} \sum_i \hat{X}_{\langle i,i+a_x\rangle}\, \hat{X}_{\langle i,i-a_x\rangle}\, \hat{X}_{\langle i,i+a_y\rangle}\, \hat{X}_{\langle i,i-a_y\rangle}. \tag{19}$$

The zero vison constraint can be satisfied with the Ansatz

$$\hat{Z}_{\langle i,j\rangle} = \hat{\tau}^z_i \hat{\tau}^z_j \quad \text{where} \quad \hat{\tau}^z = \begin{pmatrix} 1 & 0 \\ 0 & -1 \end{pmatrix}. \tag{20}$$

With this rewriting

$$\hat{X}_{\langle i,i+a_x\rangle}\, \hat{X}_{\langle i,i-a_x\rangle}\, \hat{X}_{\langle i,i+a_y\rangle}\, \hat{X}_{\langle i,i-a_y\rangle} = \hat{\tau}^x_i \quad \text{with} \quad \hat{\tau}^x = \begin{pmatrix} 0 & 1 \\ 1 & 0 \end{pmatrix}. \tag{21}$$

Hence in the zero vison sector, the unconstrained Z_2 lattice gauge theory, is given by

$$\hat{H}_{FK} = \sum_{\langle i,j\rangle,\sigma} \left(\hat{\tau}^z_i\, c^\dagger_{i,\sigma}\, \hat{\tau}^z_j\, c_{j,\sigma} + h.c. \right) - \tilde{h} \sum_i \hat{\tau}^x_i \tag{22}$$

and the local conservation law reads

$$\hat{Q}_i = \hat{X}_{\langle i,i+a_x\rangle}\, \hat{X}_{\langle i,i-a_x\rangle}\, \hat{X}_{\langle i,i+a_y\rangle}\, \hat{X}_{\langle i,i-a_y\rangle}\, (-1)^{\hat{n}^c_i} \equiv \hat{\tau}^x_i\, (-1)^{\hat{n}^c_i}. \tag{23}$$

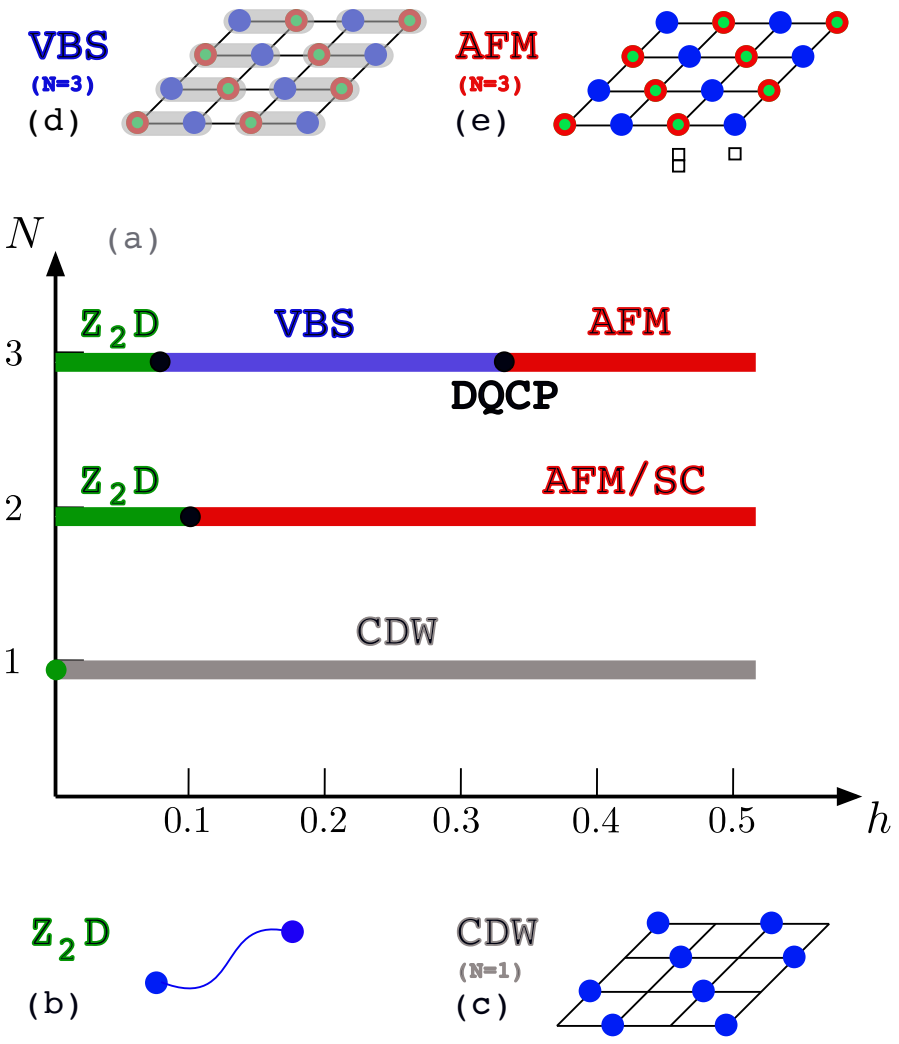

Fig. 1: *Schematic zero temperature phase diagram of the model in Eq.* (15) *in the* N *vs.* h *plane (a) as well as cartoons (b)-(e) of a selected number of phases. The fermions carry a global* $U(1)$ *electrical charge as well as a local* Z_2 *one. (a): We observe a* $\mathbb{Z}_2$ *Dirac deconfined phase (*Z_2*D), a Néel antiferromagnet phase (AFM) (or a superconductor (SC), depending on the pattern of particle-hole symmetry breaking), a charge density wave (CDW) phase as well as a valence bond solid (VBS). For* $N = 1$*, we do not find evidence for a* Z_2*D phase beyond* $h = 0$*, consistent with the arguments in the main text. The phase transitions from the* Z_2*D to AFM/SC (*$N = 2$*) and VBS (*$N = 3$*) are seemingly continuous. At* $N = 3$ *we observe a deconfined quantum critical point (DCQP) between the VBS and AFM phases. (b)-(e) Cartoons of the corresponding phases. Circles correspond to fermions and the color code to the flavor index. Circles with two colors represent a pair of fermions on a site with corresponding flavors. The low energy properties of the* Z_2*D phase resemble* $SU(N)$ *fermions propagating freely in space-time and connected by a* Z_2 *gauge string (b). The symmetry broken phases correspond to the confined phases of the model. At* $N = 3$ *the AFM phase, (e), has the fundamental (conjugate) representation of* $SU(3)$ *on sublattice A (B). The corresponding Young tableaux are included. The VBS phase, (d), corresponds to a pattern of inter-site* $SU(3)$ *singlets. This Figure is reproduced from Ref. [10].*

The explicit form of the Falikov-Kimball model can now be obtained by defining the fermion operator $\hat{f}^\dagger_{i,\sigma} = \hat{\tau}^z_i c^\dagger_{i,\sigma}$ and noting that $\hat{\tau}^x_i = \hat{Q}_i (-1)^{\hat{n}^f_i}$. Finally, since $(-1)^{\hat{n}^f_i} = \prod_\sigma (2\hat{f}^\dagger_{i,\sigma}\hat{f}_{i,\sigma} - 1)$ we obtain

$$\hat{H}_{FK} = \sum_{\langle i,j\rangle,\sigma} \left(f^\dagger_{i,\sigma} f_{j,\sigma} + h.c. \right) - \tilde{h} \sum_i \hat{Q}_i \prod_\sigma \left(2\hat{f}^\dagger_{i,\sigma}\hat{f}_{i,\sigma} - 1 \right). \tag{24}$$

Since Q_i is a Z_2 local conserved quantity, it can be interpreted as the static density of spinless fermions in a SU(N) symmetric Falikov-Kimball model [37]. A detailed study of this model shows that it harbors fractionalized orthogonal metal phases at finite temperature [44], while at low temperatures the Ising variables order ($\hat{Q}_i = 1$), such that the physics of the Hubbard model is recovered. Finally in the particle-hole symmetric case and in the limit of infinite dimensions, the model is equivalent to the Hubbard model [45, 44].

2.4 Models of fermions coupled to Ising spins

The common feature of this class of models is again to couple fermion degrees of freedom to Ising spins. However, and in contrast to the above, one will allow spontaneous Z_2 symmetry breaking such that the ordering of the Ising spins can trigger a transition in the fermionic system. This route to engineer models that can be simulated without encountering the infamous negative sign problem has recently been very successful [8–14].

The models presented in the above section have an extensive set of conserved local quantities, $\hat{Q}_i$, and as a consequence the correlation functions $\langle \hat{Z}_b \hat{Z}_{b'} \rangle$ vanishes for $b \neq b'$. In other words, there is a local Z_2 symmetry, and local symmetries cannot be broken [46]. To avoid this, one has to add terms that reduce the local Z_2 symmetry of the model from to a global one. Among many choices, one can add an Ising term of the form

$$J \sum_{\langle b,b'\rangle} \hat{Z}_b \, \hat{Z}'_b \tag{25}$$

between nearest neighbor bonds, as well as a direct hopping

$$-t \sum_b \hat{K}_b \tag{26}$$

such that the general model we will consider is given by

$$\hat{H} = \sum_b \left(-t + g\hat{Z}_b \right) \sum_{\sigma=1}^{N} \left(\hat{c}^\dagger_{i,\sigma}\hat{c}_{j,\sigma} + \hat{c}^\dagger_{j,\sigma}\hat{c}_{i,\sigma} \right) - h \sum_{\langle i,j\rangle} \hat{X}_{\langle i,j\rangle} + J \sum_{\langle b,b'\rangle} \hat{Z}_b \, \hat{Z}'_b. \tag{27}$$

The last two terms correspond to an Ising model in a transverse field. When formulating the path integral for this model, one will notice that it is identical to a $D{+}1$ Ising model,[2] albeit with space-time anisotropic couplings. Since anisotropies in the couplings are irrelevant in the sense of the renormalization group, the critical phenomena of the model fall in the $D{+}1$-dimensional Ising universality class. Coupling to gapless fermions can be relevant and lead to

[2] D corresponds to the spacial dimension

novel critical points. This idea has been successfully used to study a variety of phenomena such as the dynamical generation of quantum spin Hall [47] and Kekule mass terms [13] in Dirac systems as well as Ising nematic [48] and ferromagnetic [12] transitions in metals. This very rich set of phenomena can be studied by merely appropriately choosing the lattice, the coupling between the Ising and fermion degrees of freedom, as well as the interaction between the Ising spins.

2.5 Symmetries

The symmetries of the model will be very important to avoid the negative sign problem. In the form of Eq. (27) the SU(N) spin symmetry is manifest. On bipartite lattices this symmetry is enhanced to a O($2N$) one. To see this, we define the Majorana fermions

$$\hat{\gamma}_{i,\sigma,1} = \hat{c}_{i,\sigma} + \hat{c}^\dagger_{i,\sigma}, \quad \hat{\gamma}_{i,\sigma,2} = \frac{1}{i}\left(\hat{c}_{i,\sigma} - \hat{c}^\dagger_{i,\sigma}\right) \tag{28}$$

on sub-lattice A, and

$$\hat{\gamma}_{i,\sigma,1} = \frac{1}{i}\left(\hat{c}_{i,\sigma} - \hat{c}^\dagger_{i,\sigma}\right), \quad \hat{\gamma}_{i,\sigma,2} = -\left(\hat{c}_{i,\sigma} + \hat{c}^\dagger_{i,\sigma}\right) \tag{29}$$

on sub-lattice B. The above Majorana fermions satisfy the anti-commutation relations

$$\left\{\hat{\gamma}_{i,\sigma,n}, \hat{\gamma}_{j,\sigma',n'}\right\} = 2\delta_{i,j}\,\delta_{\sigma,\sigma'}\,\delta_{n,n'}. \tag{30}$$

Provided that the hopping matrix elements occur only between the two sub-lattices, the Hamiltonian can be written as

$$\hat{H} = \sum_{\langle i,j\rangle}\left(-t + g\,\hat{Z}_{\langle i,j\rangle}\right)\sum_{\sigma=1}^{N}\sum_{n=1}^{2}\frac{i}{2}\,\hat{\gamma}_{i,\sigma,n}\hat{\gamma}_{j,\sigma,n} - h\sum_{\langle i,j\rangle}\hat{X}_{\langle i,j\rangle} + \sum_{b.b'}J_{b,b'}\hat{Z}_b\,\hat{Z}'_b. \tag{31}$$

Here the global O($2N$) symmetry, $\hat{\gamma}_i \rightarrow O\hat{\gamma}_i$ where O corresponds to an orthogonal O($2N$) transformation and $\hat{\gamma}_i{}^T = (\hat{\gamma}_{i,1,1}\cdots\hat{\gamma}_{i,N,1}, \hat{\gamma}_{i,1,2}\cdots\hat{\gamma}_{i,N,2})$, is manifest. This symmetry plays an important role in the formulation of the negative sign free Monte Carlo algorithm.

3 General formulation of the BSS algorithm

In this section, we will show how to simulate the model of Eq. (27). It is beyond the scope of this article to offer a detailed account of the auxiliary-field QMC approach, and for a detailed review the interested reader is referred to Ref. [35]. We also note that an open-source implementation of this algorithm is available online at `https://alf.physik.uni-wuerzburg.de` [36]. This implementation allows to simulate the model defined in Eq. (27). Here we will concentrate on the general formulation and place emphasis on issues arising when considering boson-fermion problems. For the numerical stabilization of the algorithm as well as for an efficient implementation, the reader is referred to the aforementioned references.

3.1 Partition function: discrete variables

The Hilbert space of the Hamiltonian of Eq. (27) accounts for the Ising degree of freedom per bond and to N-flavored fermions per site. Thereby, the partition function reads

$$Z = \mathrm{Tr}\left(e^{-\beta \hat{H}}\right) = \mathrm{Tr}\left(\left(\prod_b e^{-\Delta\tau(-t+g\hat{Z}_b)\hat{K}_b}\right) e^{-\Delta\tau \sum_{b,b'} J_{b,b'} \hat{Z}_b \hat{Z}'_b} e^{\Delta\tau h \sum_b \hat{X}_b}\right)^{L_\tau} + \mathcal{O}\left(\Delta\tau^2\right), \tag{32}$$

where the trace runs over the fermion Fock space and the bond Ising degrees of freedom. In the above $\beta = L_\tau \Delta\tau$, and we have used an asymmetric Trotter decomposition that introduces a systematic error of order $\Delta\tau^2$.[3] We carry out the trace over the Ising variables by introducing a complete set of Ising spins on each time slice

$$\hat{Z}_b |s_1, \cdots, s_{N_b}\rangle = s_b |s_1, \cdots, s_{N_b}\rangle, \qquad \sum_{s_1,\cdots,s_{N_b}} |s_1, \cdots s_{N_b}\rangle\langle s_1, \cdots s_{N_b}| = \hat{1}_I. \tag{33}$$

Here N_b counts the number of bonds and $\hat{1}_I$ is the unit operator in the Ising space. Noting that

$$\left\langle \underline{s} \left| e^{\Delta\tau h \sum_b \hat{X}_b} \right| \underline{s}' \right\rangle = \gamma^{N_b} e^{K \sum_b s_b s'_b} \quad \text{with} \quad \tanh(K) = e^{-2\Delta\tau h}, \;\; \gamma = \frac{e^{\Delta\tau K}}{2\cosh(\Delta\tau h)} \tag{34}$$

and $|\underline{s}\rangle = |s_1, \cdots, s_{N_b}\rangle$ we obtain

$$Z = \gamma^{N_b L_\tau} \sum_{\underline{s}_1,\cdots,\underline{s}_{L_\tau}} e^{-S_0(\{\underline{s}\})} \mathrm{Tr}_F \left(\prod_{\tau,b} e^{-\Delta\tau(-t+g\, s_{b,\tau})\hat{K}_b}\right). \tag{35}$$

Here $\underline{s}$ has acquired an imaginary time index with boundary condition $\underline{s}_0 = \underline{s}_{L_\tau}$ and

$$S_0\left(\{\underline{s}\}\right) = \sum_{\tau=1}^{L_\tau} \left(\sum_{b,b'} \Delta\tau J_{b,b'} s_{b,\tau} s_{b',\tau} - K \sum_b s_{b,\tau} s_{b,\tau-1}\right). \tag{36}$$

Using the determinant formulas derived in the appendix, we can integrate out the fermions, to obtain

$$Z = \gamma^{N_b L_\tau} \sum_{\underline{s}_1,\cdots,\underline{s}_{L_\tau}} e^{-S_0(\{\underline{s}\})} \det\left(1 + \prod_{\tau,b} e^{-\Delta\tau(-t+g s_{b,\tau})K_b}\right)^N, \tag{37}$$

where the sparse matrices K_b are defined as $\hat{K}_b = \sum_{\sigma,i,j} \hat{c}^\dagger_{i,\sigma} \left(K_b\right)_{i,j} \hat{c}_{j,\sigma}$. Note that since the fermions symmetrically couple to the Ising fields $s_{b,\tau}$ the trace is block diagonal in the flavor index $\sigma = 1, \ldots, N$. Thereby we just have to compute the determinant for one flavor and elevate it to the power N. This explicitly reflects the SU(N) symmetry of our formulation.

[3] Strictly speaking the error should be of order $\Delta\tau$. However, one can show that for our specific model the coefficient of the linear in $\Delta\tau$ error vanishes [49].

3.2 From discrete to continuous fields

In the above formulation, the configuration space for the Monte Carlo sampling will corresponds to a set of discrete Ising fields. As will be apparent, it may be more efficient to consider continuous fields, for which sampling strategies such as hybrid molecular or Langevin dynamics can be used. Instead of considering the discrete Ising spin we will introduce a Gaussian transformation that formulates the problem in terms of the average magnetization. These types of transformations explicitly show the equivalence between Ising and scalar fields. We use the short hand notation

$$S_0\left(\{\underline{s}\}\right) = \frac{1}{2}\,\boldsymbol{s}^T\boldsymbol{A}\boldsymbol{s}, \tag{38}$$

where $\boldsymbol{A}$ is a $N_bL_\tau \times N_bL_\tau$ matrix and $\boldsymbol{s}^T = \left(\underline{s}_1^T, \cdots, \underline{s}_{L_\tau}^T\right)$, and will assume that $\boldsymbol{A}$ is positive definite. Here there is no loss of generality since $\boldsymbol{s}^T\boldsymbol{s} = N_bL_\tau$ such that we can add a constant to $\boldsymbol{A}$ so as to guarantee that all the eigenvalues are positive. Next we use the Gaussian identity

$$\int_{\mathbb{R}^{N_bL_\tau}} \underbrace{d\phi_1 \cdots d\phi_{N_bL_\tau}}_{\equiv D\boldsymbol{\phi}} e^{-\frac{1}{2}\boldsymbol{\phi}^T\boldsymbol{A}^{-1}\boldsymbol{\phi} - \boldsymbol{s}^T\boldsymbol{\phi}} = (2\pi)^{N_bL_\tau/2}\sqrt{\det\boldsymbol{A}}\; e^{\frac{1}{2}\boldsymbol{s}^T\boldsymbol{A}\boldsymbol{s}}. \tag{39}$$

With $C = (2\pi)^{N_bL_\tau/2}\sqrt{\det\boldsymbol{A}}$, the partition function reads

$$Z = C\int_{\mathbb{R}^{N_bL_\tau}} D\boldsymbol{\phi}\; e^{-\frac{1}{2}\boldsymbol{\phi}^T\boldsymbol{A}^{-1}\boldsymbol{\phi}}\,\mathrm{Tr}_F\left(\prod_{\tau,b}\left(\sum_{s=\pm1} e^{-s\phi_{b,\tau}}e^{-\Delta\tau(-t+gs)\hat{K}_b}\right)\right), \tag{40}$$

and we can evaluate $\sum_{s=\pm1} e^{-s\phi_{b,\tau}}\, e^{-\Delta\tau(-t+gs)\hat{K}_b}$ using the fact that $\Delta\tau$ is small

$$\begin{aligned}\sum_{s=\pm1} e^{-s\phi_{b,\tau}}\, e^{-\Delta\tau(-t+gs)\hat{K}_b} &= \sum_{s=\pm1} e^{-s\phi_{b,\tau}}\left(1-\Delta\tau(-t+gs)\hat{K}_b\right) + \mathcal{O}(\Delta\tau^2)\\ &= 2\cosh(\phi_{b,\tau})\left(1-\Delta\tau(-t+g\tanh(\phi_{b,\tau})\hat{K}_b\right) + \mathcal{O}(\Delta\tau^2)\\ &= 2\cosh(\phi_{b,\tau})\exp\left(-\Delta\tau(-t+g\tanh(\phi_{b,\tau}))\hat{K}_b\right) + \mathcal{O}(\Delta\tau^2).\end{aligned} \tag{41}$$

Thereby, the partition function can now be written as

$$Z = 2^{N_bL_\tau}C\int_{\mathbb{R}^{N_bL_\tau}} D\boldsymbol{\phi}\; e^{-\frac{1}{2}\boldsymbol{\phi}^T\boldsymbol{A}^{-1}\boldsymbol{\phi}+\sum_{b,\tau}\log\cosh(\phi_{b,\tau})}\,\mathrm{Tr}_F\left(\prod_{\tau,b} e^{-\Delta\tau(-t+g\tanh(\phi_{b,\tau}))\hat{K}_b}\right), \tag{42}$$

where we have omitted the Trotter error. Using the determinant formula for fermions, we see that

$$Z = 2^{N_bL_\tau}C\int_{\mathbb{R}^{N_bL_\tau}} D\boldsymbol{\phi}\; e^{-S(\boldsymbol{\phi})} \tag{43}$$

with

$$S(\boldsymbol{\phi}) = \frac{1}{2}\boldsymbol{\phi}^T\boldsymbol{A}^{-1}\boldsymbol{\phi} - \sum_{b,\tau}\log\cosh(\phi_{b,\tau}) - N\log\det\boldsymbol{M}(\boldsymbol{\phi}) \tag{44}$$

and

$$\boldsymbol{M}(\boldsymbol{\phi}) = 1 + \left(\prod_{\tau,b} e^{-\Delta\tau(-t+g\tanh(\phi_{b,\tau}))K_b}\right). \tag{45}$$

For future purposes, it will be useful to introduce the super-index

$$\underline{t} = (\tau, b) \tag{46}$$

that runs over the sequence of space-time bonds, and the propagators

$$\hat{U}_\phi(\underline{t}_2, \underline{t}_1) = \prod_{\underline{t}=\underline{t}_1+1}^{\underline{t}_2} e^{-\Delta\tau(-t+g\tanh(\phi_{\underline{t}}))\hat{K}_{b_{\underline{t}}}} \quad \text{for} \quad \underline{t}_2 \geq \underline{t}_1. \tag{47}$$

Note that $\hat{U}_\phi(\underline{t}, \underline{t}) = \hat{1}$.

3.3 Positivity of the determinant

An exact enumeration of the Ising spins for large euclidean volumes $N_b L_\tau$ is prohibitively expensive. A way out is to estimate the sum stochastically with importance sampling methods. This reading requires

$$P(\{\underline{s}\}) = \frac{e^{-S_0(\{\underline{s}\})} \det\left(1 + \prod_{\tau,b} e^{-\Delta\tau(-t+gs_{b,\tau})K_b}\right)^N}{\sum_{\underline{s}_1,\cdots,\underline{s}_{L_\tau}} e^{-S_0(\{\underline{s}\})} \det\left(1 + \prod_{\tau,b} e^{-\Delta\tau(-t+gs_{b,\tau})K_b}\right)^N} \tag{48}$$

to be positive. Obviously, for even values of N and since K_b are real symmetric matrices, the weight will be positive for each configuration. What about odd values of N? Using the Majorana basis introduced above, we have for a single flavor

$$\mathrm{Tr}_F \prod_{\tau,b=\langle i,j\rangle} e^{-\Delta\tau(-t+gs_{b,\tau})\left(\hat{c}_i^\dagger \hat{c}_j + \hat{c}_j^\dagger \hat{c}_i\right)} = \left(\mathrm{Tr}_M \prod_{\tau,b=\langle i,j\rangle} e^{-\Delta\tau(-t+gs_{b,\tau})\frac{i}{2}\hat{\gamma}_i\hat{\gamma}_j}\right)^2. \tag{49}$$

Here Tr_M corresponds to the trace over a single Majorana mode. We now want to show that $\mathrm{Tr}_M \prod_{\tau,b=\langle i,j\rangle} e^{-\Delta\tau(-t+gs_{b,\tau})\frac{i}{2}\hat{\gamma}_i\hat{\gamma}_j}$ is a real number

$$\overline{\mathrm{Tr}_M \prod_{\tau,b=\langle i,j\rangle} e^{-\Delta\tau(-t+gs_{b,\tau})\frac{i}{2}\hat{\gamma}_i\hat{\gamma}_j}} = \mathrm{Tr}_M \prod_{\tau,b=\langle i,j\rangle} e^{-\Delta\tau(-t+gs_{b,\tau})\frac{-i}{2}\hat{\gamma}_i\hat{\gamma}_j} = \mathrm{Tr}_M \prod_{\tau,b=\langle i,j\rangle} e^{-\Delta\tau(-t+gs_{b,\tau})\frac{i}{2}\hat{\eta}_i\hat{\eta}_j} \tag{50}$$

with

$$\hat{\eta}_i = \begin{cases} \hat{\gamma}_i & \text{for } i \in A \\ -\hat{\gamma}_i & \text{for } i \in B \end{cases} \tag{51}$$

Since the above is a canonical transformation, the trace over the $\hat{\eta}$'s is equal to that of the $\hat{\gamma}$'s. Note that we have used the fact that the hopping links only the A and B sub-lattices. Thereby the O$(2N)$ symmetry of the model allows us to show that for arbitrary number of colors $P(\{\underline{s}\})$ is positive semidefinite. For more general symmetry based arguments that lead to the absence of a negative sign problem, the reader is referred to Refs [23, 25, 26, 50]. In Appendix B we summarize some useful determinant identities for Majorana fermions. Note that the positivity of the determinant is valid for both discrete or continuous fields.

3.4 Calculation of observables

The calculation of observables proceeds as follows. Let us consider observables $\hat{O}$ that involve only fermionic degrees of freedom such that

$$\langle O \rangle = \frac{1}{\int D\boldsymbol{\phi}\, e^{-S(\boldsymbol{\phi})}} \int D\boldsymbol{\phi}\, e^{-S(\boldsymbol{\phi})}\, \frac{\mathrm{Tr}_F \left(\hat{U}_\phi(L_\tau N_b, 0)\, \hat{O} \right)}{\mathrm{Tr}_F\, \hat{U}_\phi(L_\tau N_b, 0)}. \tag{52}$$

We now consider observables of the form

$$\hat{O} = T\, \hat{c}_{i_1}(\underline{t}_1)\, \hat{c}^\dagger_{i'_1}(\underline{t}'_1) \cdots \hat{c}_{i_n}(\underline{t}_n)\, \hat{c}^\dagger_{i'_n}(\underline{t}'_n) \tag{53}$$

with

$$\hat{c}_i(\underline{t}) = \hat{U}^{-1}_\phi(\underline{t}, 0)\, \hat{c}_i\, \hat{U}_\phi(\underline{t}, 0). \tag{54}$$

In this section we omit the spin or flavor index. T corresponds to the time ordering in which the time indices, $\underline{t}$, are organized in ascending order. To achieve this ordering, one will permute operators and not forget to include the sign of the permutation in the result. For example, $T\, \hat{c}_i(\underline{1})\, \hat{c}^\dagger_j(\underline{3}) = -\hat{c}^\dagger_j(\underline{3})\, \hat{c}_i(\underline{1})$. Using the Grassmann algebra briefly introduced in Appendix A we can show that

$$\frac{\mathrm{Tr}_F \left(\hat{U}_\phi(L_\tau N_b, 0)\, \hat{O} \right)}{\mathrm{Tr}_F\, \hat{U}_\phi(L_\tau N_b, 0)} = \frac{\displaystyle\int \prod_{i,\underline{t}} d\xi^\dagger_i(\underline{t})\, d\xi_i(\underline{t})\, e^{-\sum\limits_{i,\underline{t},i',\underline{t}'} \xi^\dagger_i(\underline{t}) G^{-1}_{i,i'}(\underline{t},\underline{t}') \xi_{i'}(\underline{t}')}\, \xi_{i_1}(\underline{t}_1)\, \xi^\dagger_{i'_1}(\underline{t}'_1) \cdots \xi_{i_n}(\underline{t}_n)\, \xi^\dagger_{i'_n}(\underline{t}'_n)}{\displaystyle\int \prod_{i,\underline{t}} d\xi^\dagger_i(\underline{t})\, d\xi_i\ (\underline{t})\, e^{-\sum\limits_{i,\underline{t},i',\underline{t}'} \xi^\dagger_i(\underline{t}) G^{-1}_{i,i'}(\underline{t},\underline{t}') \xi_{i'}(\underline{t}')}}$$

$$= \det \begin{pmatrix} G_{i_1,i'_1}(\underline{t}_1, \underline{t}'_1) & \cdots & G_{i_1,i'_n}(\underline{t}_1, \underline{t}'_n) \\ \vdots & \ddots & \vdots \\ G_{i_n,i'_1}(\underline{t}_n, \underline{t}'_1) & \cdots & G_{i_n,i'_n}(\underline{t}_n, \underline{t}'_n) \end{pmatrix}. \tag{55}$$

The last equation corresponds to Wick's theorem, the demonstration of which can be found in Ref. [51]. Hence the knowledge of the Green function G is sufficient to compute any correlation function. For $\underline{t} \geq \underline{t}'$

$$G_{i,i'}(\underline{t}, \underline{t}') = \frac{\mathrm{Tr}_F \left(\hat{U}_\phi(L_\tau N_b, \underline{t})\, \hat{c}_i\, \hat{U}_\phi(\underline{t}, \underline{t}')\, \hat{c}^\dagger_{i'}\, \hat{U}_\phi(\underline{t}', 0) \right)}{\mathrm{Tr}_F\, \hat{U}_\phi(L_\tau N_b, 0)}. \tag{56}$$

Noting that

$$\hat{U}^{-1}_\phi(\underline{t}, \underline{t}')\, \hat{c}_i\, \hat{U}_\phi(\underline{t}, \underline{t}') = \sum_j B_\phi(\underline{t}, \underline{t}')_{i,j}\, \hat{c}_j \tag{57}$$

with

$$B_\phi(\underline{t}_2, \underline{t}_1) = \prod_{\underline{t}=\underline{t}_1+1}^{\underline{t}_2} e^{-\Delta\tau(-t + g \tanh(\phi_{\underline{t}})) K_{b_{\underline{t}}}} \quad \text{for} \quad \underline{t}_2 \geq \underline{t}_1, \tag{58}$$

the calculation of the imaginary time displaced Green function reduces to the calculation of the equal time one

$$
\begin{aligned}
G_{i,i'}(\underline{t}',\underline{t}') &= \frac{\mathrm{Tr}_F\left(\hat{U}_\phi(L_\tau N_b,\underline{t}')\,\hat{c}_i\,\hat{c}^\dagger_{i'}\,\hat{U}_\phi(\underline{t}',0)\right)}{\mathrm{Tr}_F\,\hat{U}_\phi(L_\tau N_b,0)} \\
&= \delta_{i,i'} - \frac{\partial}{\partial\eta}\log \mathrm{Tr}_F\left(\hat{U}_\phi(L_\tau N_b,\underline{t}')\,e^{\eta\, c^\dagger\, O^{(i',i)}\, c}\,\hat{U}_\phi(\underline{t}',0)\right)\Big|_{\eta=0}
\end{aligned}
\tag{59}
$$

with $c^\dagger\, O^{(i',i)}\, c = \hat{c}^\dagger_{i'}\hat{c}_i$. Using the determinant formula and the fact that $\det A = e^{\mathrm{Tr}\log A}$ one obtains

$$
G(\underline{t}',\underline{t}') = \left(1 + B_\phi(\underline{t}',0)\,B_\phi(L_\tau N_b,\underline{t}')\right)^{-1}. \tag{60}
$$

The equal time Green function allows to compute any equal time correlation function and as we will see it will also determine the Monte Carlo dynamics. For a given operator $\hat{O}$, we denote by $\langle\langle\hat{O}\rangle\rangle_{\boldsymbol{\phi}}$ the result of the Wick decomposition for a given field configuration $\boldsymbol{\phi}$.

3.5 Summary

All in all, we have now recast our problem into a form where importance sampling can be used. Our probability distribution

$$
P(\boldsymbol{\phi}) = \frac{e^{-S(\boldsymbol{\phi})}}{\int D\boldsymbol{\phi}\; e^{-S(\boldsymbol{\phi})}} \tag{61}
$$

is positive semi-definite and for each configuration of fields we are in the position of computing the expectation value of any operator $\hat{O}$. Our task is now to sample $P(\boldsymbol{\phi})$ so as to compute quantities of the form

$$
\langle\hat{O}\rangle = \int D\boldsymbol{\phi}\; P(\boldsymbol{\phi})\,\langle\langle\hat{O}\rangle\rangle_{\boldsymbol{\phi}}. \tag{62}
$$

4 Sampling strategies

The semi-positiveness of the determinant allows us to avoid the negative sign problem, and to thereby potentially formulate a code that scales polynomially in the Euclidean system size. However, care has to be taken with sampling strategies. We will argue below that single spin flips algorithms are bound to fail for small values of h and that a possible remedy stems from using global updating schemes such as hybrid molecular or Langevin dynamics. Both these updating schemes can only be formulated for continuous fields.

4.1 Single spin flips

Just by analyzing the form of the action, S_0, one will readily see that single spin flips are bound to be inefficient in the small h limit. The first term, $-K\sum_{b,\tau} s_{b,\tau}\, s_{b,\tau+1}$, corresponds to a one-dimensional ferromagnetic Ising model at $K = \mathrm{arctanh}\left(e^{-2\Delta\tau h}\right)$. For this problem [52] the correlation length is set by $\xi^{-1} = \log(\coth(K)) = 2\Delta\tau h$. Thereby, kinks or domain walls of

the ferromagnetic order in the imaginary time direction will be separated by a length scale set by ξ. However single spin flips produce pairs of kinks separated by the imaginary time step $\Delta\tau$ and will be very inefficient if $\Delta\tau/\xi$ is *small*. Since $\Delta\tau$ is dimension full we have to set a scale to appreciate this result. Let us consider the model of Eq. (27), and let us assume that g is the largest scale which we set to unity. We will then have to choose $\Delta\tau \ll 1$ to validate the Trotter decomposition, such that $\Delta\tau/\xi = \Delta\tau^2 h \ll 1$, and the single spin flip update will be very inefficient. This argument is based on the discreetness of the imaginary time such that with continuous time methods it may be possible to circumvent sampling issues using Ising fields.

4.2 Langevin and molecular dynamics: calculation of forces

In Langevin and hybrid molecular dynamics the key point is to compute the forces

$$\frac{\partial S(\boldsymbol{\phi})}{\partial \boldsymbol{\phi}} \tag{63}$$

and to assess if they are bounded or not. For our bosonic problems we can show explicitly that the determinant is positive semi-definite and we will make the bold assumption that it vanishes only at isolated points. Away from these isolated points, the forces will be bounded and we foresee that the Langevin and hybrid molecular dynamics walks through configuration space will be smooth. As argued in Ref. [31] this is not the case for the Hubbard model. In fact choosing a Hubbard-Stratonovich transformation that couples to the z-component of spin, splits the configuration space in distinct regions separated by logarithmic barriers where the forces diverge. For these types of landscapes formulating Langevin and hybrid molecular dynamics is very challenging. In Ref. [31] we have tested positively the above assumption for the special case of the SSH model.
Starting from the action of Eq. (44) the forces can are computed as

$$\frac{\partial S(\boldsymbol{\phi})}{\partial \phi_{\underline{t}}} = \frac{1}{2}\left(\boldsymbol{A}^{-1}\boldsymbol{\phi} + \boldsymbol{\phi}^T\boldsymbol{A}^{-1}\right)_{\underline{t}} - \tanh\phi_{\underline{t}} + Ng\Delta\tau\left(1-\tanh^2\phi_{\underline{t}}\right)\mathrm{Tr}\Big(K_{\underline{t}}(1-G(\underline{t},\underline{t}))\Big). \tag{64}$$

Here we see that the equal time Green function, $G(\underline{t},\underline{t})$, is the only fermionic quantity required to compute the forces.

4.3 Langevin dynamics

Langevin dynamics corresponds to a stochastic differential equation for the fields $\boldsymbol{\phi}$. They acquire a Langevin time t_l and satisfy the stochastic differential equation

$$\phi_{\underline{t}}(t_l + \delta t_l) = \phi_{\underline{t}}(t_l) - \frac{\partial}{\partial\phi_{\underline{t}}(t_l)} S(\boldsymbol{\phi})\,\delta t_l + \sqrt{2\,\delta t_l}\;\eta_{\underline{t}}. \tag{65}$$

Here, $\eta_{\underline{t}}$ are independent Gaussian stochastic variables satisfying

$$\langle\eta_{\underline{t}}\rangle_\eta = 0 \quad \text{and} \quad \langle\eta_{\underline{t}}\,\eta_{\underline{t}'}\rangle_\eta = \delta_{\underline{t},\underline{t}'}. \tag{66}$$

We refer the reader to Ref. [53] for a more in depth introduction to stochastic differential equations. To see that the above indeed produced the desired probability distribution in the long Langevin time limit, we can transform the Langevin equation to the corresponding Fokker-Planck equation. Let $P(\boldsymbol{\phi}, t_l)$ be the distribution of fields at Langevin time t_l. Then

$$P(\boldsymbol{\phi}, t_l + \delta t_l) = \int D\boldsymbol{\phi'}\ P(\boldsymbol{\phi'}, t_l) \left\langle \delta\left(\boldsymbol{\phi} - \left(\boldsymbol{\phi'} - \frac{\partial S(\boldsymbol{\phi'})}{\partial \boldsymbol{\phi'}}\delta t_l + \sqrt{2\delta t_l}\boldsymbol{\eta}\right)\right)\right\rangle_{\eta} \tag{67}$$

where δ corresponds to the $L_\tau N_b$ dimensional Dirac δ-function. Taylor expanding up to order δt_l and averaging over the stochastic variable yields

$$P(\boldsymbol{\phi}, t_l+\delta t_l) = \int D\boldsymbol{\phi'}\ P(\boldsymbol{\phi'}, t_l)\left(\delta(\boldsymbol{\phi'}-\boldsymbol{\phi}) - \frac{\partial S(\boldsymbol{\phi'})}{\partial \boldsymbol{\phi'}}\frac{\partial}{\partial \boldsymbol{\phi'}}\delta(\boldsymbol{\phi'}-\boldsymbol{\phi})\delta t_l + \frac{\partial}{\partial \boldsymbol{\phi'}}\frac{\partial}{\partial \boldsymbol{\phi'}}\delta(\boldsymbol{\phi'}-\boldsymbol{\phi})\delta t_l\right) + \mathcal{O}(\delta t_l^2). \tag{68}$$

Integration by parts and taking the limit of infinitesimal time steps gives the Fokker-Planck equation

$$\frac{\partial}{\partial t_l}P(\boldsymbol{\phi}, t_l) = \frac{\partial}{\partial \boldsymbol{\phi}}\left(P(\boldsymbol{\phi}, t_l)\frac{\partial S(\boldsymbol{\phi})}{\partial \boldsymbol{\phi}} + \frac{\partial P(\boldsymbol{\phi}, t_l)}{\partial \boldsymbol{\phi}}\right). \tag{69}$$

The stationary, $\frac{\partial}{\partial t_l}P(\boldsymbol{\phi}, t_l) = 0$, normalizable solution to the above equation corresponds to the desired probability distribution

$$P(\boldsymbol{\phi}) = \frac{e^{-S(\boldsymbol{\phi})}}{\int D\boldsymbol{\phi}\, e^{-S(\boldsymbol{\phi})}}. \tag{70}$$

As mentioned above, Langevin dynamics will work well provided that the forces show no singularities. The great advantage of such an updating scheme is that there is no rejection and that all fields are updated at each step. The following points that highlight potential issues with Langevin dynamics are in order:

- Langevin dynamics will be carried out at a finite Langevin time step and thereby we have introduced a further source of systematic error.
- The factor $\sqrt{2\delta t_l}$ multiplying the stochastic variable makes the noise dominant on short time scales. On these times scales Langevin dynamics essentially corresponds to a random walk. This has the advantage that one can circumvent potential barriers, but may render the updating scheme less efficient than the hybrid molecular dynamics approach.

4.4 Hybrid molecular dynamics

Hybrid molecular dynamics circumvents the aforementioned drawbacks of Langevin dynamics. It does not introduce a systematic error and does not boil down to a random walk at small time steps. The approach is based on the Metropolis-Hastings importance sampling formula. (The reader is referred to the lecture notes in Ref. [15] by the same author, where aspects of the theory of Monte Carlo sampling are discussed in Appendix A.) Let C and C' be configurations in the *Monte Carlo* space. The probability of accepting a move form C to C' is given by

$$P(C \to C') = \max\left(\frac{T_0(C' \to C)P(C')}{T_0(C \to C')P(C)}, 1\right), \tag{71}$$

where $T_0(C' \to C)$ is the probability of *proposing* a move from C' to C. In the Monte Carlo approach, we will iterate the above procedure so as to generate a time series of configurations C_m. Provided that we are able to reach all configurations in the Monte Carlo space from any starting configuration,

$$\lim_{n\to\infty} \frac{1}{n} \sum_{m=1}^{n} \delta_{C_m,C} = P(C). \tag{72}$$

Ideally, one would like to propose global, ergodic moves that satisfy $P(C \to C') = 1$ and thereby *hope* to have *small* autocorrelation times. This is a property of cluster algorithms such as the loop [35], SSE [54], or Wolff [28] algorithms.
We will start by expanding the configuration space to $C = \{\boldsymbol{p}, \boldsymbol{\phi}\}$ and define the Hamiltonian

$$H(\boldsymbol{p}, \boldsymbol{\phi}) = \frac{\boldsymbol{p}^2}{2} + S(\boldsymbol{\phi}). \tag{73}$$

$\boldsymbol{p}$ and $\boldsymbol{\phi}$ are canonical conjugate. Clearly,

$$\langle \hat{O} \rangle = \frac{\int D\boldsymbol{\phi}\, e^{-S(\boldsymbol{\phi})} \langle\langle \hat{O} \rangle\rangle_{\boldsymbol{\phi}}}{\int D\boldsymbol{\phi}\, e^{-S(\boldsymbol{\phi})}} = \frac{\int D\boldsymbol{\phi}\, D\boldsymbol{p}\; e^{-H(\boldsymbol{p},\boldsymbol{\phi})} \langle\langle \hat{O} \rangle\rangle_{\boldsymbol{\phi}}}{\int D\boldsymbol{\phi}\, D\boldsymbol{p}\; e^{-H(\boldsymbol{p},\boldsymbol{\phi})}} \tag{74}$$

and in the hybrid molecular dynamics scheme we sample

$$P(\boldsymbol{p}, \boldsymbol{\phi}) = \frac{e^{-H(\boldsymbol{p},\boldsymbol{\phi})}}{\int D\boldsymbol{\phi}\, D\boldsymbol{p}\; e^{-H(\boldsymbol{p},\boldsymbol{\phi})}}. \tag{75}$$

Hybrid molecular dynamics consists of two steps:
Step 1: Updating the momenta $\boldsymbol{p}$
Here we choose

$$T_0\left(C' = \{\boldsymbol{p}', \boldsymbol{\phi}\} \to C = \{\boldsymbol{p}, \boldsymbol{\phi}\}\right) = \frac{e^{-\boldsymbol{p}^2}}{\int d\boldsymbol{p}\; e^{-\boldsymbol{p}^2}} \tag{76}$$

such that $P(C \to C') = 1$.
Step 2: Updating the positions $\boldsymbol{\phi}$
This step is numerically expensive and uses the Hamiltonian equations of motion

$$\dot{\boldsymbol{p}} = -\frac{\partial H}{\partial \boldsymbol{\phi}} \quad \text{and} \quad \dot{\boldsymbol{\phi}} = \frac{\partial H}{\partial \boldsymbol{p}} \tag{77}$$

that conserve energy, H, for time independent Hamiltonians. As for the Langevin dynamics, the fields acquire an additional time index, t_m, and $\dot{\boldsymbol{\phi}} = \frac{d\boldsymbol{\phi}}{dt_m}$. We can propagate the fields over a given molecular dynamics time interval, T_M, to obtain

$$\{\boldsymbol{p}, \boldsymbol{\phi}\}(t_m + T_m) = U^H_{T_m}\big(\{\boldsymbol{p}, \boldsymbol{\phi}\}(t_m)\big) \tag{78}$$

where $U^H_{T_m}\big(\{\boldsymbol{p}, \boldsymbol{\phi}\}(t_m)\big)$ propagates the initial state $\{\boldsymbol{p}, \boldsymbol{\phi}\}(t_m)$ with Hamiltonian dynamics for a time interval T_m. The Hamiltonian equations of motion are time reversal symmetric and, according to Liouville's theorem, conserve volumes in phase space. Thereby,

$$\frac{T_0(\{\boldsymbol{p}, \boldsymbol{\phi}\}(t_m + T_m) \to \{\boldsymbol{p}, \boldsymbol{\phi}\}(t_m))\, e^{-H(\{\boldsymbol{p},\boldsymbol{\phi}\}(t_m+T_m))}}{T_0(\{\boldsymbol{p}, \boldsymbol{\phi}\}(t_m) \to \{\boldsymbol{p}, \boldsymbol{\phi}\}(t_m + T_m))\, e^{-H(\{\boldsymbol{p},\boldsymbol{\phi}\}(t_m))}} = 1 \tag{79}$$

and the acceptance will be of unity. Clearly this corresponds to the ideal case, and in practice the integration will be carried out with a finite time step such that the energy will not be conserved exactly and the acceptance will not be unity. Provided that we choose an integrator that is time reversal symmetric (see below) then the Monte Carlo acceptance-rejection step will cure this systematic error. The acceptance-rejection step of the molecular dynamics trajectory is the reason why this updating scheme is coined *hybrid* molecular dynamics. The algorithm then proceeds by iterating step 1 followed by step 2.

4.4.1 The leap-frog integrator

In practice one will adopt an integrator that conserves time reversal symmetry such as the Leapfrog algorithm. Our Hamiltonian can be split into $H_1 = \boldsymbol{p}^2/2$ and $H_2 = S(\boldsymbol{\phi})$. Propagating with H_1 only allows for an exact solution since in this case $\boldsymbol{p}$ is constant and $\boldsymbol{\phi}(t) = \boldsymbol{\phi}(t = t_0) + (t - t_0)\,\boldsymbol{p}$. Similarly for H_2, $\boldsymbol{\phi}$ is constant and $\boldsymbol{p}(t) = \boldsymbol{p}(t = t_0) - (t - t_0)\frac{\partial S(\boldsymbol{\phi})}{\partial \boldsymbol{\phi}}$. Hence both for H_1 and H_2 the propagation can be carried out exactly, such that time reversal symmetry and Liouville's theorem hold. In very much the same manner as for the symmetric Trotter decomposition, the leapfrog approach carries out a δt_m time interval propagation of the full Hamiltonian $H = H_1 + H_2$ as

$$U^H_{\delta t_m} = U^{H_1}_{\delta t_m/2} \circ U^{H_2}_{\delta t_m} \circ U^{H_1}_{\delta t_m/2} + \mathcal{O}\left(\delta t_m^2\right). \tag{80}$$

Clearly time reversal is satisfied and because of this property the error contains only even powers of the time step. The energy $H = H_1 + H_2$ will however not be conserved exactly such that, as mentioned above, the molecular dynamics trajectory will be accepted according to:

$$\max\left(\frac{T_0(\{\boldsymbol{p},\boldsymbol{\phi}\}(t_m + T_m) \to \{\boldsymbol{p},\boldsymbol{\phi}\}(t_m))\, e^{-H(\{\boldsymbol{p},\boldsymbol{\phi}\}(t_m+T_m))}}{T_0(\{\boldsymbol{p},\boldsymbol{\phi}\}(t_m) \to \{\boldsymbol{p},\boldsymbol{\phi}\}(t_m + T_m))\, e^{-H(\{\boldsymbol{p},\boldsymbol{\phi}\}(t_m))}}, 1\right) = \max\left(\frac{e^{-H(\{\boldsymbol{p},\boldsymbol{\phi}\}(t_m+T_m))}}{e^{-H(\{\boldsymbol{p},\boldsymbol{\phi}\}(t_m))}}, 1\right). \tag{81}$$

5 Conclusions

In these notes, we have discussed a set of very interesting boson-fermion models that are free of the negative sign problem, but that are numerically challenging due to sampling issues. The case was made that the underlying $\mathrm{O}(2N)$ symmetry of the Hamiltonians we considered render hybrid molecular dynamics an attractive sampling strategy. This statement was partially tested in Ref. [31]. More work is required to further test this conjecture that will hopefully allow us to unravel many salient aspects of a class of boson-fermion problems.

Acknowledgments

I am very indebted to S. Beyl and F. Goth who wrote a hybrid molecular dynamics code to test aspects of the conjecture presented in these notes. Many thanks to J. Hofmann, M. Hohenadler, F. Parisen Toldin, M. Raczkowski, T. Sato, J. Schwab, M. Ulybyshev, Z. Wang, M. Weber for discussions on algorithmic issues and/or on boson-fermion problems.

Appendices

A Determinant formula for fermions

In this appendix, we derive a set of so called determinant formulas for fermions. They are the basis for various forms of fermion Monte Carlo approaches and an elegant derivation is based on fermion coherent states. The reader is referred to Ref. [51] for a detailed introduction to the Grassmann algebra. Here we will briefly summarize the important formulas and concepts. Grassmann numbers, ξ, anti-commute and are defined as

$$\hat{c}_x|\xi\rangle = \xi_x|\xi\rangle \tag{82}$$

with

$$\left\{\xi_x^{\#}\ ,\xi_{x'}^{\#'}\ \right\} = \left\{\xi_x^{\#}\ ,\hat{c}_{x'}^{\#'}\right\} = 0 \tag{83}$$

and

$$|\xi\rangle = \prod_x \left(1-\xi_x\hat{c}_x^\dagger\right)|0\rangle. \tag{84}$$

In the above the subscript x denotes the quantum numbers of a single particle state and $\# = \dagger, \cdot$. Integration over Grassmann variables is defined as

$$\int d\xi_x\, \xi_x = 1\ \ , \quad \int d\xi_x = 0, \tag{85}$$

such that for example $\int d\xi_x\, d\xi_x^\dagger\ \xi_x\, \xi_x^\dagger = -1$ due to the anticommuting properties of the algebra. The following identities for overlaps

$$\langle\xi|\xi'\rangle = e^{\sum_x \xi_x^\dagger \xi_x^{'}}\,, \tag{86}$$

the resolution of unity in the Fock space

$$\hat{1} = \int \prod_x d\xi_x^\dagger\, d\xi_x\ e^{-\sum_x \xi_x^\dagger\xi_x}|\xi\rangle\langle\xi|, \tag{87}$$

and the trace over the Fock space

$$\mathrm{Tr}\,\hat{A} = \int \prod_x d\xi_x^\dagger\, d\xi_x\ e^{-\sum_x \xi_x^\dagger\xi_x}\langle -\xi|\hat{A}|\xi\rangle \tag{88}$$

hold. Finally, we will need the determinant formula

$$\int \prod_x d\xi_x^\dagger\, d\xi_x\ e^{-\sum_{x,y}\xi_x^\dagger M_{x,y}\xi_y} = \det M. \tag{89}$$

As mentioned above, these formulas are *standard* and can be found in Ref. [51].
Our aim is compute

$$\mathrm{Tr}\left(e^{\hat{c}^\dagger A_n\hat{c}}\ e^{\hat{c}^\dagger A_2\hat{c}}\ \cdots e^{\hat{c}^\dagger A_1\hat{c}}\ \right), \tag{90}$$

where $\hat{c}^\dagger = (\hat{c}_1^\dagger, \cdots, \hat{c}_{N_s}^\dagger)$ with N_s the number of single particle states. The first step is to transform $e^{\hat{c}^\dagger A \hat{c}}$ into a normal ordered expression. We will see that for a general A

$$e^{\hat{c}^\dagger A \hat{c}} = : e^{\hat{c}^\dagger \left(e^A - 1\right) \hat{c}} : , \tag{91}$$

where $: \hat{O} :$ denotes the normal ordering of the operator $\hat{O}$. To prove the above, we diagonalize A: $\lambda = UAU^{-1}$, with λ a diagonal matrix, and define $\hat{\eta}^\dagger = \hat{c}^\dagger U$ and $\hat{\gamma} = U^{-1}\hat{c}$. These operators satisfy the anti-commutations rules

$$\left\{\hat{\eta}_x^\dagger, \hat{\gamma}_y\right\} = \delta_{x,y}, \quad \text{and} \quad \left\{\hat{\eta}_x^\dagger, \hat{\eta}_y^\dagger\right\} = \left\{\hat{\gamma}_x, \hat{\gamma}_y\right\} = 0 \tag{92}$$

such that

$$e^{\hat{c}^\dagger A \hat{c}} = \prod_x e^{\lambda_x \hat{\eta}_x^\dagger \hat{\gamma}_x} = \prod_x \left(1 + (e^{\lambda_x} - 1)\hat{\eta}_x^\dagger \hat{\gamma}_x\right) = \prod_x : e^{\hat{\eta}_x^\dagger (e^{\lambda_x} - 1)\hat{\gamma}_x} : = : e^{\sum_x \hat{\eta}_x^\dagger (e^{\lambda_x} - 1)\hat{\gamma}_x} : = : e^{\hat{c}^\dagger (e^A - 1)\hat{c}} : . \tag{93}$$

With the above, we can evaluate the matrix element

$$\langle \xi | e^{\hat{c}^\dagger A \hat{c}} \, | \xi' \rangle = e^{\xi^\dagger (e^A - 1)\xi'} \langle \xi | \xi' \rangle = e^{\xi^\dagger (e^A)\xi'} . \tag{94}$$

Using the Grassmann trace formula and inserting the resolution of unity between the operators, we obtain

$$\begin{aligned} \mathrm{Tr}\left(e^{\hat{c}^\dagger A_n \hat{c}} \, \cdots e^{\hat{c}^\dagger A_2 \hat{c}} \, e^{\hat{c}^\dagger A_1 \hat{c}} \right) &= \int \prod_{x,\tau=1}^{n} d\xi_x^\dagger(\tau) \, d\xi_x(\tau) \; e^{-\left(\sum_{x,\tau=1}^n \xi_x^\dagger(\tau)\xi_x(\tau) - \sum_{\tau=1}^n \xi^\dagger(\tau+1) e^{A_\tau} \xi(\tau) \right)} \\ &= \int \prod_{x,\tau=1}^{n} d\xi_x^\dagger(\tau) \, d\xi_x(\tau) e^{-\xi_x^\dagger(\tau) \, G^{-1}_{(x,\tau),(x',\tau')} \, \xi_{x'}(\tau')} . \end{aligned} \tag{95}$$

In the above, the Grassmann fields have acquired an extra dimension τ and we have defined $\xi_x^\dagger(n+1) = -\xi_x^\dagger(1)$. Finally with the determinant formula we can integrate over the Grassmann variables and obtain

$$\mathrm{Tr}\left(e^{\hat{c}^\dagger A_n \hat{c}} \, \cdots e^{\hat{c}^\dagger A_2 \hat{c}} \, e^{\hat{c}^\dagger A_1 \hat{c}} \right) = \det \begin{pmatrix} 1 & 0 & \cdots & 0 & e^{A_n} \\ -e^{A_2} & 1 & \cdots & 0 & 0 \\ \vdots & & \ddots & \cdots & 0 \\ 0 & \cdots & \cdots & -e^{A_{n-1}} & 1 \end{pmatrix} . \tag{96}$$

The size of the this matrix is of $nN_s \times nN_s$, and is the starting point for many applications in the realm of the so called hybrid QMC approaches used in the high energy community. For many applications in the solid state, it is more convenient to reduce the size of the matrix down to $N_s \times N_s$. This can be achieved with Schur's determinant identity

$$\det \begin{pmatrix} A & B \\ C & D \end{pmatrix} = \det(D) \det(A - BD^{-1}C) \tag{97}$$

Setting $D = 1$, corresponding to the bottom right unity matrix, $C = (0, \cdots, -e^{-A_{n-1}})$ and $B^T = (e^{A_n}, \cdots 0)$ gives

$$\det \begin{pmatrix} 1 & 0 & \cdots & 0 & e^{A_n} \\ -e^{A_2} & 1 & \cdots & 0 & 0 \\ \vdots & & \ddots & \cdots & 0 \\ 0 & \cdots & \cdots & -e^{A_{n-1}} & 1 \end{pmatrix} = \det \begin{pmatrix} 1 & 0 & \cdots & 0 & e^{A_n} e^{A_{n-1}} \\ -e^{A_2} & 1 & \cdots & 0 & 0 \\ \vdots & & \ddots & \cdots & 0 \\ 0 & \cdots & \cdots & -e^{A_{n-2}} & 1 \end{pmatrix}. \quad (98)$$

Iteration produces the final result

$$\mathrm{Tr}\left(e^{\hat{c}^\dagger A_n \hat{c}} \cdots e^{\hat{c}^\dagger A_2 \hat{c}} \, e^{\hat{c}^\dagger A_1 \hat{c}} \right) = \det\left(1 + e^{A_n} \cdots e^{A_2} e^{A_1}\right). \quad (99)$$

B Determinant formula for Majoranas

Here we will prove the following identity

$$\mathrm{Tr}_M\left(e^{i\hat{\gamma}^T T_1 \hat{\gamma}} \cdots e^{i\hat{\gamma}^T T_L \hat{\gamma}} \right) = \sqrt{\det(1 + e^{4iT_1} \cdots e^{4iT_L})}, \quad (100)$$

where T_τ are skew symmetric real matrices of even dimension ($T_\tau^T = -T_\tau$), and $\hat{\gamma}^T = (\hat{\gamma}_{1,1}, \hat{\gamma}_{1,2} \cdots, \hat{\gamma}_{n,1}, \hat{\gamma}_{n,2})$ are Majorana fermions.
First, we show that one can find an antisymmetric matrix h that satisfies

$$e^{i\hat{\gamma}^T T_1 \hat{\gamma}} \cdots e^{i\hat{\gamma}^T T_{L_\tau} \hat{\gamma}} = e^{i\hat{\gamma}^T h \hat{\gamma}}. \quad (101)$$

The above follows from the fact that, using the anti-commutation rules of Majorana fermions,

$$\frac{d}{d\tau} \underbrace{e^{-i\tau\hat{\gamma}^T T \hat{\gamma}} \, \hat{\gamma}_i \, e^{i\tau\hat{\gamma}^T T \hat{\gamma}}}_{\equiv \hat{\gamma}_i(\tau)} = 4i \sum_j T_{i,j} \hat{\gamma}_j(\tau) \quad (102)$$

such that

$$\hat{\gamma}(\tau) = e^{4i\tau T} \hat{\gamma}. \quad (103)$$

Iteration gives

$$e^{-i\hat{\gamma}^T T_L \hat{\gamma}} \cdots e^{-i\hat{\gamma}^T T_1 \hat{\gamma}} \, \hat{\gamma} \, e^{i\hat{\gamma}^T T_1 \hat{\gamma}} \cdots e^{i\hat{\gamma}^T T_L \hat{\gamma}} = e^{4iT_1} \cdots e^{4iT_L} \hat{\gamma} \equiv e^{-i\hat{\gamma}^T h \hat{\gamma}} \, \hat{\gamma}_i \, e^{i\hat{\gamma}^T h \hat{\gamma}}. \quad (104)$$

The last equality is the defining equation for h and leads to

$$e^{4iT_1} \cdots e^{4iT_L} = e^{4ih}. \quad (105)$$

That h is skew symmetric stems from the fact that, by definition, $e^{4ih} \left(e^{4ih}\right)^T = 1$. We will proceed by assuming that h is a real skew symmetric matrix.[4] Thereby one can find an orthogonal transformation O such that

$$O^T h O = \mathrm{diag}\left(\begin{pmatrix} 0 & \lambda_1 \\ -\lambda_1 & 0 \end{pmatrix}, \cdots, \begin{pmatrix} 0 & \lambda_n \\ -\lambda_n & 0 \end{pmatrix} \right) \equiv \lambda. \quad (106)$$

[4] A generalization to complex skew symmetric matrices is mentioned in Ref. [50]

Since O is orthogonal, $\hat{\eta} \equiv O^T \hat{\gamma}$ are Majorana fermions and

$$\mathrm{Tr}_M e^{i\hat{\gamma}^T\, h\, \hat{\gamma}} = \mathrm{Tr}_M e^{i\hat{\gamma}^T\, O\, \lambda\, O^T\, \hat{\gamma}} = \mathrm{Tr}_M \prod_{i=1}^{n} e^{2i\lambda_i\, \hat{\eta}_{i,1}\, \hat{\eta}_{i,2}} = \mathrm{Tr}_M \prod_{i=1}^{n} \Big(\cosh(2\lambda_i) + \sinh(2\lambda_i) \hat{\eta}_{i,1}\, \hat{\eta}_{i,2} \Big). \tag{107}$$

We can now *refermionize* the Majorana operators

$$\hat{\eta}_{i,1} = \hat{c}_i + \hat{c}_i^\dagger \quad , \quad \hat{\eta}_{i,2} = \frac{1}{i}(\hat{c}_i - \hat{c}_i^\dagger), \tag{108}$$

and carry out the trace for each fermion flavor, to obtain

$$\begin{aligned} \mathrm{Tr}_M e^{i\hat{\gamma}^T h \hat{\gamma}} &= \mathrm{Tr}_F \prod_{i=1}^{n} \Big(\cosh(2\lambda_i) + \sinh(2\lambda_i) \frac{1}{i} (2\hat{c}_i^\dagger \hat{c}_i - 1) \Big) \\ &= \prod_{i=1}^{n} 2\cosh(2\lambda_i) = \left(\prod_{i}^{n} \left(e^{4\lambda_i} + e^{-4\lambda_i} + 2 \right) \right)^{1/2} = \Big(\det(1 + e^{4iO^T h O}) \Big)^{1/2} \\ &= \Big(\det(1 + e^{4ih}) \Big)^{1/2} = \Big(\det(1 + e^{4iT_1} \cdots e^{4iT_L}) \Big)^{1/2}. \end{aligned} \tag{109}$$

References

[1] J. Bardeen, L.N. Cooper, and J.R. Schrieffer, Phys. Rev. **108**, 1175 (1957)

[2] A. Migdal, JETP **34**, 996 (1958)

[3] G. Eliashberg, JETP **11**, 696 (1960)

[4] P.A. Lee, T.M. Rice, J.W. Serene, L.J. Sham, and J.W. Wilkins, Comm. Condens. Matter Phys. **12**, 99 (1986)

[5] M. Hohenadler and H. Fehske, ArXiv:1706.00470 (2017)

[6] W.P. Su, J.R. Schrieffer, and A.J. Heeger, Phys. Rev. B **22**, 2099 (1980)

[7] A.P. Schnyder, S. Ryu, A. Furusaki, and A.W.W. Ludwig, Phys. Rev. B **78**, 195125 (2008)

[8] E. Berg, M.A. Metlitski, and S. Sachdev, Science **338**, 1606 (2012)

[9] Y. Schattner, S. Lederer, S.A. Kivelson, and E. Berg, ArXiv e-prints (2015)

[10] F.F. Assaad and T. Grover, Phys. Rev. X **6**, 041049 (2016)

[11] S. Gazit, M. Randeria, and A. Vishwanath, Nat. Phys. **13**, 484 (2017)

[12] X.Y. Xu, K. Sun, Y. Schattner, E. Berg, and Z.Y. Meng, Phys. Rev. X **7**, 031058 (2017)

[13] T. Sato, M. Hohenadler, and F.F. Assaad, Phys. Rev. Lett. **119**, 197203 (2017)

[14] S. Gazit, F.F. Assaad, S. Sachdev, A. Vishwanath, and C. Wang, ArXiv:1804.01095 (2018)

[15] F.F. Assaad: *Continuous-Time QMC Solvers for Electronic Systems in Fermionic and Bosonic Baths*, in E. Pavarini, E. Koch, D. Vollhardt, A. Lichtenstein (eds.): *DMFT at 25: Infinite Dimensions*, Modeling and Simulation Vol. 4 (Forschungszentrum Jülich, 2014)

[16] A.N. Rubtsov, V.V. Savkin, and A.I. Lichtenstein, Phys. Rev. B **72**, 035122 (2005)

[17] F.F. Assaad and T.C. Lang, Phys. Rev. B **76**, 035116 (2007)

[18] M. Hohenadler, F.F. Assaad, and H. Fehske, Phys. Rev. Lett. **109**, 116407 (2012)

[19] M. Hohenadler, Phys. Rev. Lett. **117**, 206404 (2016)

[20] M. Weber, F.F. Assaad, and M. Hohenadler, Phys. Rev. B **94**, 245138 (2016)

[21] M. Weber, F.F. Assaad, and M. Hohenadler, Phys. Rev. Lett. **119**, 097401 (2017)

[22] M. Weber and M. Hohenadler, ArXiv:1709.01096 (2017)

[23] C. Wu and S.-C. Zhang, Phys. Rev. B **71**, 155115 (2005)

[24] E.F. Huffman and S. Chandrasekharan, Phys. Rev. B **89**, 111101 (2014)

[25] Z.-X. Li, Y.-F. Jiang, and H. Yao, Phys. Rev. Lett. **117**, 267002 (2016)

[26] Z.C. Wei, C. Wu, Y. Li, S. Zhang, and T. Xiang, Phys. Rev. Lett. **116**, 250601 (2016)

[27] M. Hohenadler and T.C. Lang, in H. Fehske, R. Schneider, and A. Weisse (eds.): *Computational Many-Particle Physics* (Springer-Verlag, Heidelberg, 2008), pp. 357–366

[28] U. Wolff, Phys. Rev. Lett. **62**, 361 (1989)

[29] C. Chen, X.Y. Xu, J. Liu, G. Batrouni, R. Scalettar, and Z.Y. Meng, ArXiv:1802.06177 (2018)

[30] C. Zhang, B. Shahbaba, and H. Zhao, ArXiv:1506.05555 (2015)

[31] S. Beyl, F. Goth, and F.F. Assaad, Phys. Rev. B **97**, 085144 (2018)

[32] R. Blankenbecler, D.J. Scalapino, and R.L. Sugar, Phys. Rev. D **24**, 2278 (1981)

[33] S. Duane and J.B. Kogut, Phys. Rev. Lett. **55**, 2774 (1985)

[34] S. Duane, A.D. Kennedy, B.J. Pendleton, and D. Roweth, Phys. Lett. **B195**, 216 (1987)

[35] F. Assaad and H. Evertz, in H. Fehske, R. Schneider, and A. Weiße (eds.): *Computational Many-Particle Physics* (Springer, Heidelberg, 2008), pp. 277–356

[36] M. Bercx, F. Goth, J.S. Hofmann, and F.F. Assaad, SciPost Phys. **3**, 013 (2017)

[37] L.M. Falicov and J.C. Kimball, Phys. Rev. Lett. **22**, 997 (1969)

[38] M. Weber, F.F. Assaad, and M. Hohenadler, Phys. Rev. B **91**, 245147 (2015)

[39] E. Zohar, J.I. Cirac, and B. Reznik, Rep. Prog. Phys. **79**, 014401 (2016)

[40] C. Prosko, S.-P. Lee, and J. Maciejko, Phys. Rev. B **96**, 205104 (2017)

[41] A. Smith, D.L. Kovrizhin, R. Moessner, and J. Knolle, ArXiv:1803.06575 (2018)

[42] W. Metzner, M. Salmhofer, C. Honerkamp, V. Meden, and K. Schönhammer, Rev. Mod. Phys. **84**, 299 (2012)

[43] E.H. Lieb, Phys. Rev. Lett. **73**, 2158 (1994)

[44] M. Hohenadler and F.F. Assaad, ArXiv:1804.05858 (2018)

[45] R. Žitko and M. Fabrizio, Phys. Rev. B **91**, 245130 (2015)

[46] S. Elitzur, Phys. Rev. D **12**, 3978 (1975)

[47] Y.-Y. He, X.Y. Xu, K. Sun, F.F. Assaad, Z.Y. Meng, and Z.-Y. Lu, Phys. Rev. B **97**, 081110 (2018)

[48] Y. Schattner, S. Lederer, S.A. Kivelson, and E. Berg, Phys. Rev. X **6**, 031028 (2016)

[49] R.M. Fye, Phys. Rev. B **33**, 6271 (1986)

[50] Z.-C. Wei, ArXiv:1712.09412 (2017)

[51] J.W. Negele and H. Orland: *Quantum Many body systems* (Addison-Wesley, 1988)

[52] R.J. Baxter: *Exactly solved models in statistical mechanics* (Academic Press, London, 1989)

[53] C.W. Gardiner: *Handbook of Stochastic Methods* (Springer, 1985)

[54] A.W. Sandvik, Phys. Rev. B **59**, R14157 (1999)